

Phenomenological aspects of composite Higgs scenarios: exotic scalars and vector-like quarks

A. BANERJEE¹, D. BUARQUE FRANZOSI², G. CACCIAPAGLIA³, A. DEANDREA³,
G. FERRETTI¹, T. FLACKE⁴, B. FUKS⁵, M. KUNKEL⁶, L. PANIZZI⁷, W. POROD⁶,
L. SCHWARZE⁶

¹ *Department of Physics, Chalmers University of Technology, Fysikgården, 41296
Göteborg, Sweden*

² *Stockholm University, Department of Physics, 106 91 Stockholm, Sweden*

³ *Univ. Lyon, Université Claude Bernard Lyon 1, CNRS/IN2P3, IP2I UMR5822,
F-69622, Villeurbanne, France*

⁴ *Center for AI and Natural Sciences, KIAS, Seoul 02455, Korea*

⁵ *Laboratoire de Physique Théorique et Hautes Energies (LPTHE), UMR 7589, Sorbonne
Université et CNRS, 4 place Jussieu, 75252 Paris Cedex 05, France*

⁶ *Institut für Theoretische Physik und Astrophysik, Uni Würzburg, Emil-Hilb-Weg 22,
D-97074 Würzburg, Germany*

⁷ *Department of Physics and Astronomy, Uppsala University, Box 516, SE-751 20
Uppsala, Sweden*

Submitted to the Proceedings of the US Community Study
on the Future of Particle Physics (Snowmass 2021)

ABSTRACT

Composite Higgs models usually contain additional pseudo Nambu Goldstone bosons and vector-like quarks. We discuss various aspects related to their LHC phenomenology and provide summary plots of exclusion limits using currently available information. We also describe a general parametrisation implemented in a software for Monte Carlo simulations and study the $SU(5)/SO(5)$ scenario as a concrete example.

Contents

1	Executive summary	2
2	Composite Higgs and partial compositeness: an outline	3
3	LHC bounds for pair production of pNGBs and VLQs	5
4	Case study: $SU(5)/SO(5)$	10
A	The general Lagrangian for models with VLQs and pNGBs	12

1 Executive summary

Models of electroweak (EW) symmetry breaking by a composite Higgs [1] with partial compositeness [2] in the top-quark sector give promising solutions to the hierarchy problem [3–7] of the Standard Model (SM). At the effective field theory level they can be described by specifying the pattern of symmetry breaking involved. Generically these models predict the existence of light scalars in addition to the Higgs boson, all emerging as pseudo Nambu-Goldstone bosons (pNGBs). Partial compositeness also implies the presence of vector-like quarks (VLQs). This proliferation of new particles requires a systematic approach to study this class of models and to facilitate a seamless transition between theory, data, and simulation codes.

Current experimental analyses already allow to set limits on the masses of such particles in specific scenarios depending on their interactions. For pNGBs, we provide an overview plot of the limits for pair production cross-sections times branching ratios in various final states (Fig. 2). We also work out a concrete example based on the $SU(5)/SO(5)$ coset (Fig. 7). For VLQs, we emphasize the relevance of their exotic decays by presenting a plot summarizing current limits in the VLQ mass versus pNGB mass plane (Fig. 4).

Furthermore, we provide a general parametrisation describing the interactions of the new particles arising in composite scenarios, which can be used for phenomenological studies and is implemented in a numerical model for Monte Carlo simulations [8]. A software toolbox of a new kind is also being developed, `FSMOG` (`FeynRules` plugin for Simplified MOdel Generation) [9], to automatize the construction of the most general interaction Lagrangian given a specific particle content, which has a much wider range of applications beyond the realm of composite Higgs models.

2 Composite Higgs and partial compositeness: an outline

There are many approaches to strongly-coupled EW symmetry breaking scenarios [4–7]. The most investigated ones include, e.g., 5D holographic theories [10] and multi-site deconstructed models like Little Higgs models [11]. Instead of using the holographic duality, we consider directly a class of composite Higgs models based on 4D asymptotically free (hypercolor) gauge theories. We assume that the hypercolor theory, after going through a near conformal running [12, 13], confines at the multi-TeV scale. To include top partial compositeness, its fundamental degrees of freedom contain fermionic matter in two inequivalent irreducible representations (irreps) of hypercolor [14, 15], chosen in order to sequester the EW coset from the composite states carrying QCD color.

The strong sector is associated with a global symmetry \mathcal{G} that breaks spontaneously to a subgroup \mathcal{H} below the confinement scale, such that the SM gauge symmetry is contained in the unbroken subgroup \mathcal{H} . The symmetry breaking pattern induced by the fermionic condensates gives rise to an EW coset containing the Higgs boson as a pNGB. The three minimal cosets arising from real, pseudoreal and complex irreps, containing at least a pNGB Higgs doublet and preserving custodial symmetry, are $SU(5)/SO(5)$ [16, 17] (real), $SU(4)/Sp(4)$ [18, 19] (pseudoreal), and $SU(4) \times SU(4)'/SU(4)_D$ [20, 21] (complex), respectively. Holographic/little Higgs constructions, reviewed in [4] and [11], lead to additional cosets, for instance the well-known minimal model $SO(5)/SO(4)$ (MCHM) [3] or $SO(6)/SO(4) \times SO(2)$ [22]. Most of the low energy phenomenology discussed here is also applicable to this wider variety of models. Below the condensation scale, the colored VLQs originate from the trilinear fermionic operators combining the two irreps in a hypercolor invariant way. They are assumed to mix linearly with the SM quarks of the third generation through partial compositeness. We do not review these constructions here but refer to the existing literature: see [14, 15] for the initial constructions (a streamlined classification can be found in [23]). Additional models of this type are presented in [17, 24–32].

Composite Higgs models have two major types of experimental signatures in the low energy range. First, the pNGB nature of the Higgs boson implies modifications of its couplings with the other SM particles [33–37]. The other kind of signature involves additional particles beyond the SM (BSM), predicted by these models, for example, exotic EW pNGBs [23, 38–40], colored pNGBs [39, 41], VLQs [42–48] and other colored fermionic states in non-triplet irreps [49], vector resonances [50–54], and axion-like particles [55, 56]. In this contribution we focus on EW pNGBs and exotic decay modes of VLQs.

To construct the low energy theory [57, 58] involving the pNGBs of the EW sector, the VLQs, and the SM quarks and gauge bosons one must choose a symmetry breaking pattern \mathcal{G}/\mathcal{H} , VLQs in \mathcal{H} irreps, and an embedding of the SM quarks into an irrep of \mathcal{G} , see [6, 42, 59–61] for detailed constructions.

Fields	Spin	$SU(3)_c$	$U(1)_{\text{em}}$
S_i^0	0	1	0
S_i^\pm	0	1	± 1
$S_i^{\pm\pm}$	0	1	± 2
π_r^q	0	r	q
T	1/2	3	2/3
B	1/2	3	-1/3
X	1/2	3	5/3

Table 1: BSM particle content considered in the Lagrangian presented in this section. For the colored scalars π_r^q , the subscript $r = \mathbf{3}, \mathbf{6}, \mathbf{8}$ denotes the $SU(3)_c$ representation. We allow for multiple colorless scalars $S_i^{0,\pm,\pm\pm}$ ($i = 1, 2, \dots$) since they generically arise in composite Higgs models.

2.1 A general parametrisation

Here and in the appendix we present the generic Lagrangian, focusing on the interactions of the pNGBs and the VLQs. At this stage we only use invariance under the electromagnetic $U(1)_{\text{em}}$ and the QCD color $SU(3)_c$ to construct the interactions. This introduces a large number of arbitrary couplings that will have to be fixed in a specific model implementation. We take this approach since it can be easily implemented in software tools.

We consider the particle content shown in Tab. 1. As mentioned above, even this choice reflects some restrictions on the type of degrees of freedom present. However, this field content is sufficient for the discussion below. The interaction Lagrangian can be expressed as follows

$$\begin{aligned} \mathcal{L}_{\text{int}} = & \mathcal{L}_{SSV} + \mathcal{L}_{SSVV} + \mathcal{L}_{SVV} + \mathcal{L}_{SV\tilde{V}} + \mathcal{L}_{\Psi\Psi V} + \mathcal{L}_{\Psi f V} + \mathcal{L}_{\Psi f S} + \mathcal{L}_{ffS} \\ & + \mathcal{L}_{\pi\pi V + \pi\pi VV} + \mathcal{L}_{\pi V\tilde{V}} + \mathcal{L}_{\Psi f\pi} + \mathcal{L}_{ff\pi}, \end{aligned} \quad (1)$$

where $\Psi \equiv \{T, B, X\}$ collectively denotes the VLQs. In addition to the field content in Tab. 1, V and f denote the SM gauge bosons and third generation quarks. The explicit expressions for each term of the above Lagrangian are presented in the appendix.

For the time being, we use a `FeynRules` implementation of the above Lagrangian, limited to the EW pNGBs, and VLQs [8], through which a UFO model [62] has been generated. The UFO implementation allows the simulation of processes up to one-loop in QCD. A more automatized tool, `FSMOG` (`FeynRules` plugin for Simplified MOdel Generation), is being developed to facilitate the writing of the most general Lagrangian. The program will take as input fields of given spin, charge, and color and output the `FeynRules` file containing the most general interactions between these fields and the SM ones, up to a certain mass dimension. At present this is limited to dimension-4 operators for simplicity, however future

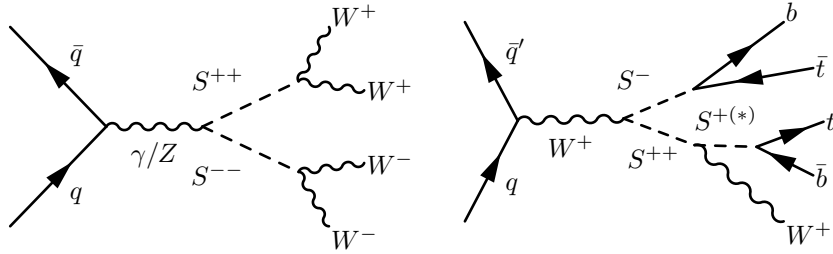


Figure 1: Examples of pNGB pair production via Drell-Yan processes with subsequent decays into SM particles.

versions of FSMOG will include commonly used higher dimension operators. FSMOG is still under development, but the current version can be obtained from the authors [9]. In this implementation the reduction of number of independent couplings for a specific model is achieved by using a `FeynRules`-style restriction card.

3 LHC bounds for pair production of pNGBs and VLQs

3.1 Electroweak pNGBs

In this section we confine ourselves to the case where the only accessible degrees of freedom are the pNGBs from the EW coset. We present the bounds on their production cross sections times branching ratios as function of their mass in various channels. In this way, the bounds are applicable to any BSM scenario with scalars.

The direct production of EW pNGBs can occur either via Drell-Yan processes or via vector boson fusion. In case of pair production the Drell-Yan processes

$$pp \rightarrow S_i^{\pm\pm} S_j^{\mp}, S_i^{\pm} S_j^0, S_i^{++} S_j^{--}, S_i^{+} S_j^{-}, S_i^0 S_j^0 \quad (2)$$

clearly dominate. The vector boson fusion processes also allow single production via the anomaly induced couplings, see Eq. (11) in the appendix. However, the corresponding cross sections are rather small as these couplings are loop induced. Nevertheless, these couplings become important for the pNGB decays if couplings to SM fermions are either forbidden or strongly suppressed. In this case the dominant decays are

$$S_i^{++} \rightarrow W^{+}W^{+} \quad (3a)$$

$$S_i^{+} \rightarrow W^{+}\gamma, W^{+}Z \quad (3b)$$

$$S_i^0 \rightarrow W^{+}W^{-}, \gamma\gamma, \gamma Z, ZZ. \quad (3c)$$

Combining these with the various production channels leads to a plethora of final states containing 4 gauge bosons, see for example left diagram in Fig. 1. A few of these processes have been searched for directly: Ref. [63] sets bounds on the cross section times branching ratio of $S^{++}S^{--} \rightarrow WWWW$ and $S^{\pm\pm}S^{\mp} \rightarrow WWWW$, which are included in Fig. 2.

Contur pool	Description	final state(s)
ATLAS-13-LL-GAMMA	dilepton and ≥ 1 photon [64]	$W\gamma W\gamma$,
ATLAS-13-GAMMA	inclusive multiphotons [65]	$W\gamma W\gamma$, $W\gamma WZ$ $W\gamma\gamma\gamma$
ATLAS-13-GAMMA-MET	photon and MET [66]	$W\gamma WZ$
ATLAS-13-4L	four leptons [67]	$WZWZ$
ATLAS-13-L1L2METJET	unlike dilepton, MET and jets [68]	$W\gamma W\gamma$, $WZWZ$
ATLAS-13-MMJET	$\mu^+\mu^-$ at the Z pole, plus optional jets [69]	$WZWZ$
CMS-13-EEJET	e^+e^- at the Z pole, plus optional jets [70]	$WZWZ$
CMS-13-MMJET	$\mu^+\mu^-$ at the Z pole, plus optional jets [70]	$WZWZ$

Table 2: Contur pools that are most sensitive to the final states listed in the last column.

Given a coset, the anomaly couplings of pNGBs to vector bosons are fixed up to an overall constant, while the couplings to fermions are more model-dependent. It is typically possible to construct both fermiophobic as well as fermiophilic models. If present, the couplings of pNGBs to quarks in Eq. (17) of the appendix are expected to scale with m_q/f , i.e.

$$\kappa_t^{S_i^0} \sim \frac{m_t}{f}, \quad \kappa_b^{S_i^0} \sim \frac{m_b}{f}, \quad \kappa_{tb,L/R}^{S_i^+} \sim \frac{m_t}{f}, \quad (4)$$

up to factors of order 1, where f is the pNGB decay constant. In this case the branching ratios into third-generation quarks dominate over the loop-induced anomaly decays into vector bosons. The corresponding decay channels are

$$S^{++} \rightarrow W^+ t\bar{b}, \quad (5a)$$

$$S^+ \rightarrow t\bar{b}, \quad (5b)$$

$$S^0 \rightarrow t\bar{t}, b\bar{b}. \quad (5c)$$

Note that the three-body decay $S^{++} \rightarrow W^+ t\bar{b}$ proceeds via an off-shell S^+ , see right diagram in Fig. 1. To our knowledge, this channel has not been studied in the literature before. The corresponding branching ratio is usually close to 100% as the decay $S^{++} \rightarrow W^+ W^+$ is loop-induced. In this section we assume that all pNGBs have the same mass. Effects induced due to mass differences are more model-dependent, hence we defer the corresponding discussion to Sec. 4 for a specific model.

We determine the extent to which the currently recasted analyses can constrain processes for which no direct searches exist. To this end, we have implemented simplified models in `FeynRules` [71] at leading order. We have generated 10^5 events using `MadGraph5_aMC@NLO` [72] version 3.3.1 with the `NPDF 2.3` set of parton densities [73, 74] and hadronized them with `Pythia8` [75]. To obtain constraints on the parameter space, the events are analysed with `MadAnalysis5`, [76–79] version 1.9.60. `MadAnalysis5` performs an event reconstruction using `Delphes 3` [80] and the anti- k_T algorithm [81] implemented in `FastJet` [82], and calculates an exclusion using the CL_s prescription [83]. We also tested the generated events

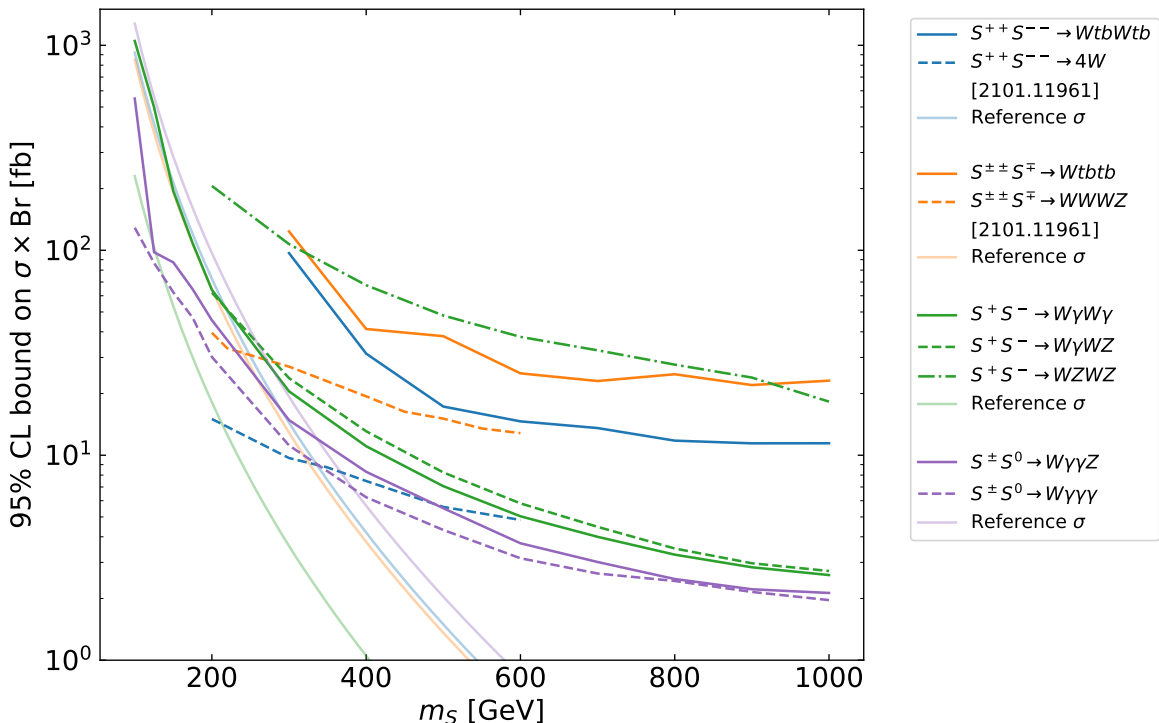


Figure 2: Upper limits on the cross section times branching ratio of the Drell-Yan production of electroweak pNGBs. The bounds are obtained from recasts implemented in `Contur` and `MadAnalysis5` except for the ones presented in [63]. The reference cross sections σ for pair production are calculated for a custodial quintuplet from a benchmark model that is discussed in detail in Sec. 4.

against the SM measurements implemented in `Rivet` [84] version 3.1.5 and have calculated exclusions from the respective YODA files with `Contur` [85, 86]. Here, we have used all available analyses in `Contur` version 2.1.1, as well as Refs. [65, 66, 87] from the upcoming release 2.2.1.

For final states with quarks (in particular top quarks) we found BSM searches implemented in `MadAnalysis5` to be the most constraining.* In contrast, in case of vector boson final states, we obtain the bounds in general from measurements implemented in `Rivet`, on which `Contur` is based. In Fig. 2 we present the bounds on the pair-production cross section times branching ratio for various final states. Beyond our recast results, we also included the results of the ATLAS search for $pp \rightarrow S^{++}S^{--} \rightarrow WWWW$ and $pp \rightarrow S^{\pm\pm}S^{\mp} \rightarrow WWWZ$ [63] for completeness. In Tab. 2 we give the most sensitive `Contur` pools for the various vector boson final states. In the case of quark final states the strongest bounds stem from the four-top search CMS-TOP-18-003 [90], which is implemented in `MadAnalysis5` [91].

For reference, in Fig. 2 we also show the production cross section for members of a

*An analysis using BSM searches implemented in `CheckMATE` [88, 89] is in preparation.

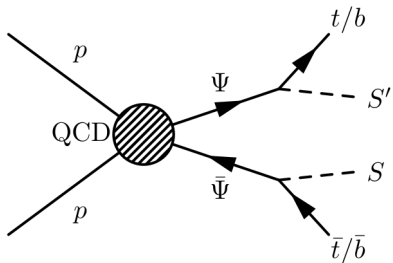


Figure 3: Illustration of VLQ pair production with subsequent decays into pNGBs and third generation quarks.

custodial quintuplet, which is part of the benchmark scenario based on the $SU(5)/SO(5)$ coset discussed in Sec. 4. Note that the references are production cross sections, while the bounds shown are constraints on $\sigma \times \text{Br}$. To obtain bounds on m_S , these reference cross sections must be multiplied by the (model-dependent) branching ratios into the respective final states. Comparing the theoretical cross sections to the obtained constraints, it is clear that the currently implemented analyses can give bounds on m_S of at most 400 GeV (in the $S^\mp S^0$ -channel, if the respective branching ratios to $W\gamma$ and $\gamma\gamma$ are close to 1). We want to stress that other models give cross section of the same size. For example, the cross sections shown for $S^{++}S^{--}$ and $S^{\pm\pm}S^\mp$ are the same as for the $SU(2)_L$ triplet used in the ATLAS analysis [63]. The main model dependence enters not in the pair production cross section but in the branching ratios of the pNGB decays.

3.2 Vector-like quarks

Coloured particles have a privileged role in the determination of model-independent constraints from searches at the LHC, since the cross-section of QCD pair production depends exclusively on their masses. VLQs have been extensively searched at the LHC by both ATLAS and CMS, under the general assumption that the SM is minimally extended with one VLQ, directly decaying into SM final states. Strong bounds on their masses (above the TeV) have been obtained regardless of their decay channels [92–103].

We have seen, however, that in the scenarios at hand VLQs can also interact with further lighter exotic states, such as new pNGBs, changing their decay patterns as indicated in Fig. 3. Exclusion bounds obtained under the aforementioned hypotheses thus require a reinterpretation to account for the reduced branching ratios into SM final states. Moreover, the new decay channels can be tested against experimental data to obtain combined limits on the masses of VLQs and the new states they can decay into. Experimental searches targeting exotic decays of VLQs are not available yet, however phenomenological analyses providing recasts of different searches have already appeared [44, 104–113].

A summary of results from some of these analyses, corresponding to exclusive decays (100% Br) of the VLQs into different exotic states, is presented in Fig. 4. When additional decay channels are open, bounds on VLQ masses can be significantly lower than those

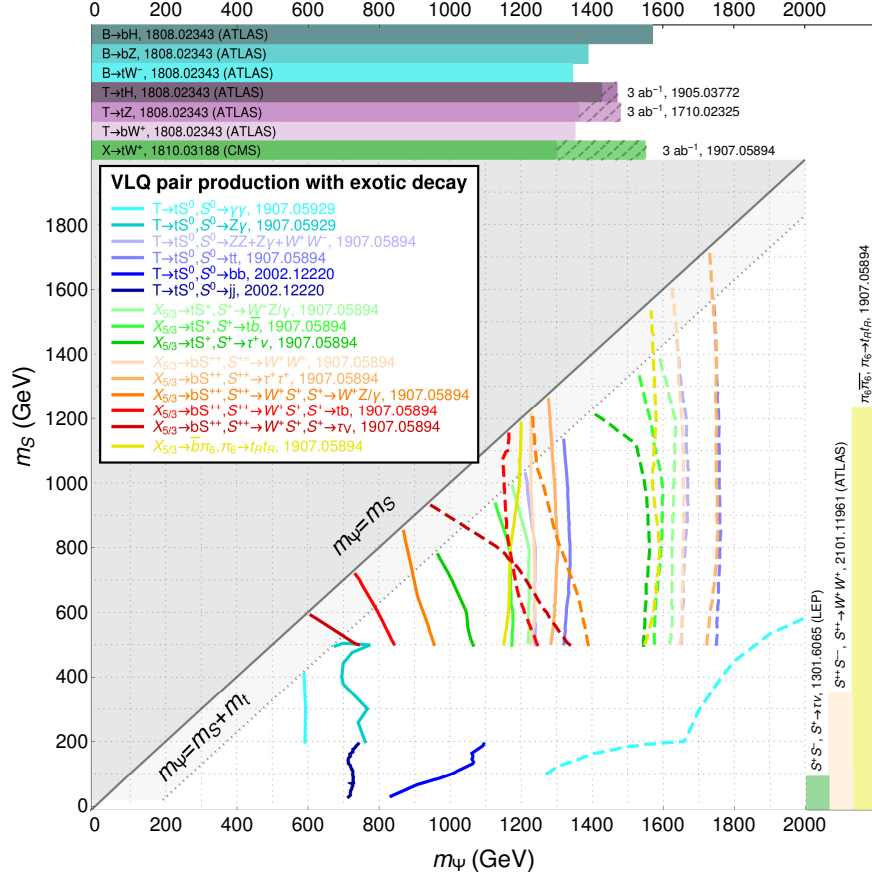


Figure 4: 95% CL limits in the $\{m_\Psi, m_S\}$ plane for VLQs decaying to new pNGBs. Current bounds (13 TeV , 36 fb^{-1}) are shown by the solid lines while the projections for the high luminosity LHC (3 ab^{-1}) are shown in dashed lines (for details, see corresponding references). Current experimental bounds on the masses of VLQs decaying to SM particles only and the masses of spin-0 states produced in pairs are provided as horizontal and vertical bars respectively. The hatched regions in the bars denote projections for 3 ab^{-1} luminosity.

reported in current experimental searches. In this case, results from Fig. 4 should be accompanied by maps of experimental efficiencies or upper limits on the cross-sections in the same plane for each relevant decay channel of the VLQ.[†] The representation proposed in Fig. 4 has thus the purpose to provide an overview and a general reference for where realistic bounds can be placed. We also present the projected exclusions in the same channels for high luminosity LHC (3 ab^{-1}) [44, 106].

To allow an easy comparison with experimental results, current bounds (and future projections for some cases) on the masses of VLQs decaying to SM particles and bounds on the masses of pair-produced pNGBs have also been included as horizontal [100, 114–116] and vertical [63, 117, 118] bars respectively. Notice that except for the colour sextet π_6 , a residual

[†]An explicit example of this kind of analysis has been proposed in [46] for pair production of $X_{5/3}$ decaying to light leptons, not motivated by composite scenarios.

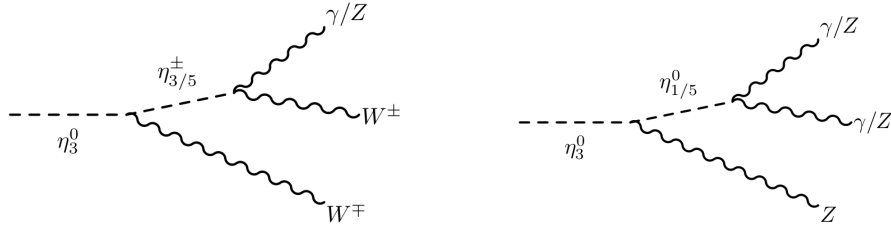


Figure 5: Feynman diagrams corresponding to three-body decays of η_3^0 .

model dependence affects the exclusion limits: the pair production cross-section of an EW pNGB depends on its coupling to the Z boson, which is associated with its representation under the EW gauge group. Experimental bounds on charged scalars are obtained under specific assumptions, for which we refer to the corresponding literature [63, 117, 118].

4 Case study: $SU(5)/SO(5)$

As a concrete example, we now consider a model based on the $SU(5)/SO(5)$ coset after having integrated out the VLQs. The UV theory can be constructed as in [17] and it's being studied on the lattice [119, 120]. This coset delivers a total of 14 pNGBs, which include the Higgs bidoublet, a singlet η , and a bitriplet under $SU(2)_L \times SU(2)_R$. Here we focus on the bitriplet, as direct η production at the LHC is strongly suppressed. The bitriplet decomposes as a quintuplet $\eta_5 \equiv (\eta_5^0, \eta_5^\pm, \eta_5^{\pm\pm})$, a triplet $\eta_3 \equiv (\eta_3^0, \eta_3^\pm)$ and a singlet η_1^0 of custodial $SU(2)_C$.

A detailed description of how all the couplings can be derived, including the VLQ sector, has been given in [61]. For this section we consider the exotic pNGBs to be fermiophobic. In Appendix A.1, we collect the relevant couplings, which depend on the pNGB decay constant f , which we set to 1 TeV. The remaining parameters to be chosen are the masses for the custodial multiplets $m_{1,3,5}$ [‡]. Note that the exotic pNGBs do not acquire a vacuum expectation value in this model.

In this scenario, these pNGBs are mainly produced through Drell-Yan processes (see Eq. (2)). In the presence of a mass splitting between the custodial multiplets the decay pattern changes with respect to the discussion in Sec. 3. In such case the lowest lying multiplet will still decay only via the anomaly. However, the heavier pNGBs will decay dominantly into a possibly off-shell vector boson and a member of the lower lying multiplet, as soon as the mass splitting is larger than about 1 GeV. As an example we take $m_3 \geq m_{5,1}$,

[‡]In principle members of different custodial multiplets can mix as discussed in [40].

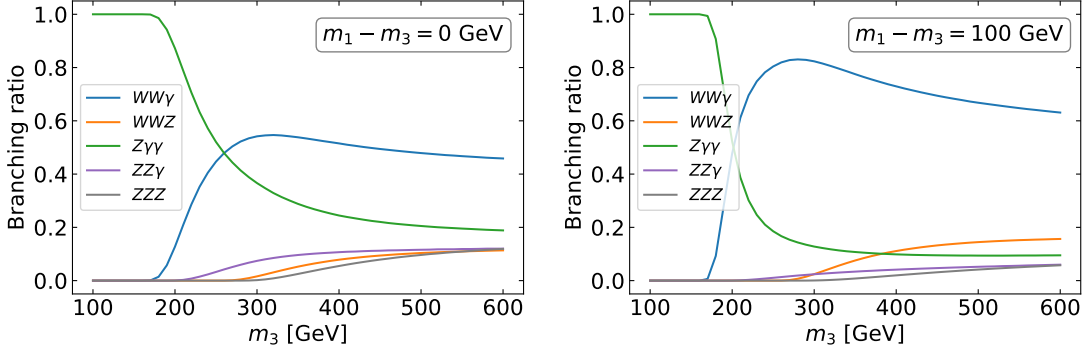


Figure 6: Three-body decays of η_3^0 for the scenario $m_{1,3} \ll m_5$. When kinematically accessible, the dominant channel is $\eta_3^0 \rightarrow W^\pm \eta_3^{\mp(*)}$.

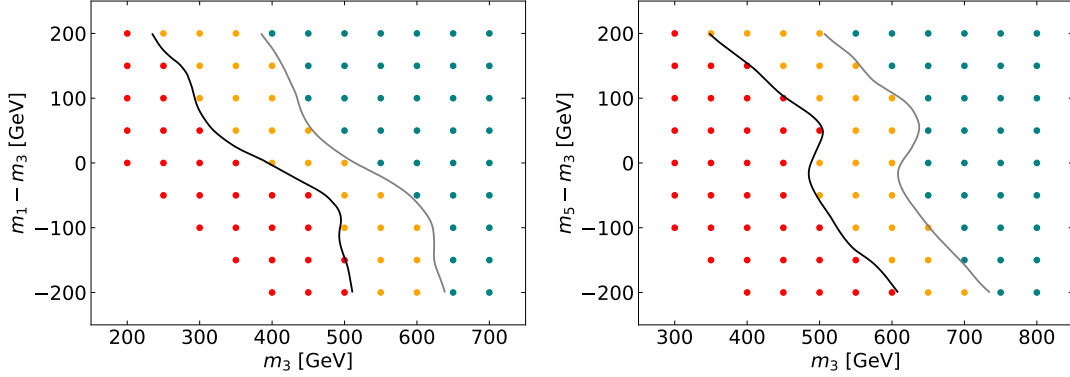


Figure 7: Exclusion bounds on the pNGB masses in $m_3 - \Delta m$ plane, where $\Delta m = m_1 - m_3$ (left panel) and $\Delta m = m_5 - m_3$ plane (right panel). In both cases we assume the pNGBs are fermiophobic and produced in pair through Drell-Yan processes. The black (grey) lines represent the $2\text{-}\sigma$ ($1\text{-}\sigma$) exclusion. Red points are excluded with CL above $2\text{-}\sigma$ and yellow ones between 1 and $2\text{-}\sigma$.

in which case the η_3 members decay dominantly as

$$\begin{aligned} \eta_3^+ &\rightarrow \eta_5^{++} W^{-(*)}, \eta_5^+ Z^{(*)}, \eta_5^0 W^{+(*)}, \eta_1^0 W^{+(*)}; \\ \eta_3^0 &\rightarrow \eta_5^\pm W^{\mp(*)}, \eta_5^0 Z^{(*)}, \eta_1^0 Z^{(*)}. \end{aligned} \quad (6)$$

Since $\Gamma_{\eta_{5,1}} \ll \Gamma_{W,Z}$, the decays into off-shell $\eta_{5,1}$ and on-shell vector bosons are strongly suppressed. Note that in scenarios where η_3 is the lightest multiplet, η_3^0 is forced to have three body decays since it does not couple to the anomaly, see Fig. 5. We give examples of branching ratios of η_3^0 for different scenarios in Fig. 6. We use the same set-up as in Sec. 3 to determine bounds at the LHC, assuming a global K -factor of 1.15 to take QCD corrections into account. We find again that **Contur** yields stronger bounds than currently available analyses in **MadAnalysis5**. The leading bounds are displayed in Fig. 7 for two limiting scenarios: $m_{1,3} \ll m_5$ (left plot) and $m_{3,5} \ll m_1$ (right plot). The bounds on the right side are much stronger due to the presence of the additional singly and doubly charged states in the quintuplet.

Acknowledgements

We thank Jon Butterworth for helpful discussions on `Contur`. A.B., D.B.F., G.F. and L.P. acknowledge support from the Knut and Alice Wallenberg foundation under the grant KAW 2017.0100 (SHIFT project). G.C., A.D., M.K, W.P. and L.S. have been supported by the “DAAD, Frankreich” and “Partenariat Hubert Curien (PHC)” PROCOPE 2021-2023, project number 57561441. T.F, M.K., W.P and L.S were supported under the framework of the international cooperation program “GenKo” managed by the National Research Foundation of Korea (No. 2022K2A9A2A15000153, FY2022) and DAAD, P33 - projekt-id 57608518. G.C., A.D., T.F. and B.F. acknowledge support from the Campus-France STAR project n. 43566UG, “Higgs and Dark Matter connections”. T.F. is supported by KIAS Individual Grant (AP083701) via the Center for AI and Natural Sciences at Korea Institute for Advanced Study. G.C. and A.D. are grateful to the LABEX Lyon Institute of Origins (ANR-10-LABX-0066) Lyon for its financial support within the program “Investissements d’Avenir” of the French government operated by the National Research Agency (ANR).

A The general Lagrangian for models with VLQs and pNGBs

In this appendix we provide the explicit expressions of each of the terms shown in Eq. (1) which is also implemented in the software tools, albeit with a limited particle content. The terms \mathcal{L}_{SSV} , \mathcal{L}_{SSVV} , and $\mathcal{L}_{\pi\pi V+\pi\pi VV}$ are simply the couplings of the pNGBs with the gauge bosons, arising from the covariant derivative.

$$\begin{aligned}
\mathcal{L}_{SSV} = & \frac{ie}{s_W} W^{-\mu} \sum_{i,j} \left[K_W^{S_i^0 S_j^+} S_i^0 \overleftrightarrow{\partial}_\mu S_j^+ + K_W^{S_i^- S_j^{++}} S_i^- \overleftrightarrow{\partial}_\mu S_j^{++} \right] + \text{h.c.} \\
& + \frac{ie}{s_W c_W} Z^\mu \left[\sum_{i<j} K_Z^{S_i^0 S_j^0} S_i^0 \overleftrightarrow{\partial}_\mu S_j^0 + \sum_{i,j} \left(K_Z^{S_i^+ S_j^-} S_i^+ \overleftrightarrow{\partial}_\mu S_j^- + K_Z^{S_i^{++} S_j^{--}} S_i^{++} \overleftrightarrow{\partial}_\mu S_j^{--} \right) \right] \\
& - ie A^\mu \sum_i \left[S_i^+ \overleftrightarrow{\partial}_\mu S_i^- + 2S_i^{++} \overleftrightarrow{\partial}_\mu S_i^{--} \right], \tag{7}
\end{aligned}$$

$$\begin{aligned}
\mathcal{L}_{SSVV} = & e^2 A_\mu A^\mu \sum_i [S_i^+ S_i^- + 4S_i^{++} S_i^{--}] \\
& + \frac{e^2}{s_W c_W} A^\mu Z_\mu \sum_{i,j} \left[K_{AZ}^{S_i^+ S_j^-} S_i^+ S_j^- + K_{AZ}^{S_i^{++} S_j^{--}} S_i^{++} S_j^{--} \right] \\
& + \frac{e^2}{s_W^2 c_W^2} Z_\mu Z^\mu \left[\sum_{i \leq j} K_{ZZ}^{S_i^0 S_j^0} S_i^0 S_j^0 + \sum_{i,j} \left(K_{ZZ}^{S_i^+ S_j^-} S_i^+ S_j^- + K_{ZZ}^{S_i^{++} S_j^{--}} S_i^{++} S_j^{--} \right) \right] \\
& + \frac{e^2}{s_W^2} W_\mu^+ W^{-\mu} \left[\sum_{i \leq j} K_{WW}^{S_i^0 S_j^0} S_i^0 S_j^0 + \sum_{i,j} \left(K_{WW}^{S_i^+ S_j^-} S_i^+ S_j^- + K_{WW}^{S_i^{++} S_j^{--}} S_i^{++} S_j^{--} \right) \right] \\
& + \frac{e^2}{s_W} A^\mu W_\mu^- \sum_{i,j} \left[K_{AW^-}^{S_i^0 S_j^+} S_i^0 S_j^+ + K_{AW^-}^{S_i^- S_j^{++}} S_i^- S_j^{++} \right] + \text{h.c.} \\
& + \frac{e^2}{s_W^2 c_W} Z^\mu W_\mu^- \sum_{i,j} \left[K_{ZW^-}^{S_i^0 S_j^+} S_i^0 S_j^+ + K_{ZW^-}^{S_i^- S_j^{++}} S_i^- S_j^{++} \right] + \text{h.c.} \\
& + \frac{e^2}{s_W^2} W_\mu^- W^{-\mu} \left[\sum_{i \leq j} K_{W^- W^-}^{S_i^+ S_j^+} S_i^+ S_j^+ + \sum_{i,j} \left(K_{W^- W^-}^{S_i^0 S_j^{++}} S_i^0 S_j^{++} \right) \right] + \text{h.c.}, \tag{8}
\end{aligned}$$

$$\mathcal{L}_{\pi\pi V + \pi\pi VV} = \sum_{r=3,6,8} (D_\mu \pi_r^q)^\dagger D^\mu \pi_r^q, \tag{9}$$

with $D_\mu = \partial_\mu - ig_s G^{a\mu} T_r^a - ieq(A_\mu - \tan \theta_W Z_\mu)$ and $s_W(c_W) \equiv \sin \theta_W(\cos \theta_W)$. Note that the colored pNGBs do not carry any $SU(2)_L$ index in the models considered here and, thus, the couplings to the Z arise purely from hypercharge. The \mathcal{L}_{SVV} consists of the coupling of the Higgs boson to the EW gauge bosons.

$$\mathcal{L}_{SVV} = 2M_W^2 \frac{h}{v} \left[K_{WW}^h W_\mu^+ W^{-\mu} + K_{ZZ}^h \frac{1}{2c_W^2} Z_\mu Z^\mu \right]. \tag{10}$$

Any additional pNGB acquiring a vacuum expectation value contributes to the masses of the gauge bosons and acquires a coupling of this type. We consider here the case where only the Higgs doublet receives a vacuum expectation value (v). In this case, the neutral scalars easily evade all LEP collider bounds and no corrections to the tree-level ρ -parameter arise. This choice is well motivated by a study of the potential for models given in [23, 40].

The Lagrangian $\mathcal{L}_{SV\tilde{V}}$ and $\mathcal{L}_{\pi V\tilde{V}}$ contain the dimension five anomalous couplings of the pNGBs with the vector boson field strengths. If one proceeds to integrate out the third family or the heavy vector bosons, both \mathcal{L}_{SVV} and $\mathcal{L}_{SV\tilde{V}}$ include additional dimension five

couplings such as the coupling of the Higgs boson to the gluons.

$$\begin{aligned}
\mathcal{L}_{SV\tilde{V}} = & \frac{e^2}{16\pi^2 v} \left[\sum_i S_i^0 \left(\tilde{K}_{\gamma\gamma}^{S_i^0} F_{\mu\nu} \tilde{F}^{\mu\nu} + \frac{2}{s_W c_W} \tilde{K}_{\gamma Z}^{S_i^0} F_{\mu\nu} \tilde{Z}^{\mu\nu} + \frac{1}{s_W^2 c_W^2} \tilde{K}_{ZZ}^{S_i^0} Z_{\mu\nu} \tilde{Z}^{\mu\nu} \right. \right. \\
& + \left. \frac{2}{s_W^2} \tilde{K}_{WW}^{S_i^0} W_{\mu\nu}^+ \tilde{W}^{-\mu\nu} \right) + \sum_i S_i^+ \left(\frac{2}{s_W} \tilde{K}_{\gamma W}^{S_i^+} F_{\mu\nu} \tilde{W}^{-\mu\nu} + \frac{2}{s_W^2 c_W} \tilde{K}_{ZW}^{S_i^+} Z_{\mu\nu} \tilde{W}^{-\mu\nu} \right) + \text{h.c.} \\
& + \left. \frac{1}{s_W^2} \sum_i S_i^{++} \tilde{K}_{W^-W^-}^{S_i^{++}} W_{\mu\nu}^- \tilde{W}^{-\mu\nu} + \text{h.c.} \right], \tag{11}
\end{aligned}$$

$$\mathcal{L}_{\pi V\tilde{V}} = \frac{1}{16\pi^2 f} \left(g_s^2 \tilde{K}_{gg}^{\pi_8^0} \pi_8^0 G_{\mu\nu} \tilde{G}^{\mu\nu} + 2g_s e \tilde{K}_{g\gamma}^{\pi_8^0} \pi_8^0 G_{\mu\nu} \tilde{F}^{\mu\nu} + \frac{2g_s e}{s_W c_W} \tilde{K}_{gZ}^{\pi_8^0} \pi_8^0 G_{\mu\nu} \tilde{Z}^{\mu\nu} \right). \tag{12}$$

The only terms in $\mathcal{L}_{\Psi\Psi V}$ relevant for VLQ pair production are their couplings to the gluons

$$\mathcal{L}_{\Psi\Psi V} = \frac{g_s}{2} [\bar{T}\mathcal{G}^a \lambda^a T + \bar{B}\mathcal{G}^a \lambda^a B + \bar{X}\mathcal{G}^a \lambda^a X], \tag{13}$$

with λ^a being the usual Gell-Mann matrices. The terms $\mathcal{L}_{\Psi f V}$, $\mathcal{L}_{\Psi f S}$, and $\mathcal{L}_{\Psi f \pi}$ arise from partial compositeness by linearly coupling the VLQs (Ψ) to the third quark family (f).

$$\begin{aligned}
\mathcal{L}_{\Psi f V} = & \frac{e}{\sqrt{2}s_W} \kappa_{T,L}^W \bar{T} W^+ P_L b + \frac{e}{2c_W s_W} \kappa_{T,L}^Z \bar{T} Z P_L t + \frac{e}{\sqrt{2}s_W} \kappa_{B,L}^W \bar{B} W^- P_L t \\
& + \frac{e}{2c_W s_W} \kappa_{B,L}^Z \bar{B} Z P_L b + \frac{e}{\sqrt{2}s_W} \kappa_{X,L}^W \bar{X} W^+ P_L t + L \leftrightarrow R + \text{h.c.} \tag{14}
\end{aligned}$$

$$\begin{aligned}
\mathcal{L}_{\Psi f S} = & \sum_i S_i^+ \left[\kappa_{T,L}^{S_i^+} \bar{T} P_L b + \kappa_{X,L}^{S_i^+} \bar{X} P_L t + L \leftrightarrow R \right] + \text{h.c.} + \sum_i S_i^- \left[\kappa_{B,L}^{S_i^-} \bar{B} P_L t + L \leftrightarrow R \right] + \text{h.c.} \\
& + \sum_i S_i^0 \left[\kappa_{T,L}^{S_i^0} \bar{T} P_L t + \kappa_{B,L}^{S_i^0} \bar{B} P_L b + L \leftrightarrow R \right] + \text{h.c.} \\
& + \sum_i S_i^{++} \left[\kappa_{X,L}^{S_i^{++}} \bar{X} P_L b + L \leftrightarrow R \right] + \text{h.c.} \tag{15}
\end{aligned}$$

$$\begin{aligned}
\mathcal{L}_{\Psi f \pi} = & \pi_8^0 \left[\kappa_{T,L}^{\pi_8^0} \bar{T} P_L t + \kappa_{B,L}^{\pi_8^0} \bar{B} P_L b + L \leftrightarrow R \right] + \text{h.c.} \\
& + \left[\pi_6^{4/3} \left(\kappa_{T,L}^{\pi_6^{4/3}} \bar{T} C P_R \bar{t}^T + \kappa_{X,L}^{\pi_6^{4/3}} \bar{X} C P_R \bar{b}^T \right) + \pi_6^{2/3} \kappa_{B,L}^{\pi_6^{2/3}} B^T C P_L b + L \leftrightarrow R \right] + \text{h.c.} \tag{16}
\end{aligned}$$

with C being the charge conjugation operator. The terms \mathcal{L}_{ffS} and $\mathcal{L}_{ff\pi}$ involving two SM third generation quarks are given below with $y_f = \sqrt{2}m_f/v$.

$$\begin{aligned}
\mathcal{L}_{ffS} = & -\frac{h}{\sqrt{2}} \left[y_t \kappa_t^h \bar{t} t + y_b \kappa_b^h \bar{b} b \right] + \sum_i S_i^0 \left[\bar{t} \left(\kappa_t^{S_i^0} + i\tilde{\kappa}_t^{S_i^0} \gamma_5 \right) t + \bar{b} \left(\kappa_b^{S_i^0} + i\tilde{\kappa}_b^{S_i^0} \gamma_5 \right) b \right] \\
& + \sum_i S_i^+ \left[\kappa_{tb,L}^{S_i^+} \bar{t} P_L b + L \leftrightarrow R \right] + \text{h.c.} \tag{17}
\end{aligned}$$

Fields in Eq. (1)	Fields in section 4
S_i^0	$h, \eta, \eta_1^0, \eta_3^0, \eta_5^0$
S_i^\pm	η_3^\pm, η_5^\pm
$S_i^{\pm\pm}$	$\eta_5^{\pm\pm}$

Table 3: Mapping between the generic symbols for the spin-0 fields to the specific EW pNGBs in the custodial basis for $SU(5)/SO(5)$ coset

$$\begin{aligned}
\mathcal{L}_{ff\pi} = & \pi_8^0 \left[\bar{t}(\kappa_t^{\pi_8^0} + i\tilde{\kappa}_t^{\pi_8^0}\gamma_5)t + \bar{b}(\kappa_b^{\pi_8^0} + i\tilde{\kappa}_b^{\pi_8^0}\gamma_5)b \right] \\
& + \pi_6^{4/3}\bar{t}(\kappa_t^{\pi_6^{4/3}} + i\tilde{\kappa}_t^{\pi_6^{4/3}}\gamma_5)C\bar{t}^T + \pi_6^{2/3}b^T(\kappa_b^{\pi_6^{2/3}} + i\tilde{\kappa}_b^{\pi_6^{2/3}}\gamma_5)Cb + \text{h.c.} \quad (18)
\end{aligned}$$

A.1 Couplings in $SU(5)/SO(5)$ coset

Now we present the explicit coupling strengths between the weak gauge bosons and EW pNGBs in the custodial basis for $SU(5)/SO(5)$ coset, in terms of $\sin\theta \equiv s_\theta = v/f$. The couplings presented below can be directly used to construct the restriction cards for the Feynrules-based tools we discussed earlier. In Tab. 3 we map the generic symbols for the scalar fields used in the Eq. (1) to the specific symbols used for the $SU(5)/SO(5)$ coset. The coefficient K_{VV}^h ($V = W, Z$), the universal modification of the Higgs coupling with the weak gauge bosons appearing in \mathcal{L}_{SVV} is given by c_θ .

Coefficients appearing in \mathcal{L}_{SSV}

$K_W^{S_i^0 S_j^+}$			$K_Z^{S_i^0 S_j^0}$				$K_Z^{S_i^+ S_j^-}$			$K_Z^{S_i^{++} S_j^{--}}$
η_3^+	η_5^+	η_5^{++}	h	η_3^0	η_5^0	η_1^0	η	η_3^-	η_5^-	η_5^{--}
h	0	0	h	0	0	0	0			
η_3^0	$-\frac{i}{2}$	$\frac{c_\theta}{2}$	η_3^0	0	$\frac{ic_\theta}{\sqrt{3}}$	$i\sqrt{\frac{2}{3}}c_\theta$	0			
η_5^0	$-\frac{c_\theta}{2\sqrt{3}}$	$\frac{i\sqrt{3}}{2}$	η_5^0		0	0	0	-		-
η_1^0	$\sqrt{\frac{2}{3}}c_\theta$	0	η_1^0			0	0			
η	0	0	η				0			
η_3^-	-	$\frac{c_\theta}{\sqrt{2}}$	η_3^+					$-\frac{c_{2W}}{2}$	$-\frac{ic_\theta}{2}$	
η_5^-		$-\frac{i}{\sqrt{2}}$	η_5^+						$-\frac{c_{2W}}{2}$	
			η_5^{++}				-			$-c_{2W}$

Coefficients appearing in \mathcal{L}_{SSVV}

	$K_{ZZ}^{S_i^0 S_j^0}$					$K_{ZZ}^{S_i^+ S_j^-}$		$K_{ZZ}^{S_i^{++} S_j^{--}}$
	h	η_3^0	η_5^0	η_1^0	η	η_3^-	η_5^-	η_5^{--}
h	$\frac{c_{2\theta}}{8}$	0	0	0	0			
η_3^0		$\frac{3+5c_{2\theta}}{16}$	0	0	0			
η_5^0			$\frac{c_{2\theta}}{6}$	$\frac{3+5c_{2\theta}}{12\sqrt{2}}$	$-\sqrt{\frac{5}{6}} \frac{s_\theta^2}{2}$	—		—
η_1^0				$\frac{15+17c_{2\theta}}{96}$	$-\sqrt{\frac{5}{3}} \frac{s_\theta^2}{8}$			
η					$-\frac{5s_\theta^2}{16}$			
η_3^+			—			$\frac{3-2s_{2W}^2+c_{2\theta}}{8}$	$\frac{ic_{2W}c_\theta}{2}$	
η_5^+							$\frac{c_{2W}^2+c_{2\theta}}{4}$	
η_5^{++}				—				c_{2W}^2

	$K_{WW}^{S_i^0 S_j^0}$					$K_{WW}^{S_i^+ S_j^-}$		$K_{WW}^{S_i^{++} S_j^{--}}$
	h	η_3^0	η_5^0	η_1^0	η	η_3^-	η_5^-	η_5^{--}
h	$\frac{c_{2\theta}}{4}$	0	0	0	0			
η_3^0		$\frac{3+c_{2\theta}}{8}$	0	0	0			
η_5^0			$\frac{9+c_{2\theta}}{12}$	$-\frac{3+5c_{2\theta}}{12\sqrt{2}}$	$\sqrt{\frac{5}{6}} \frac{s_\theta^2}{2}$	—		—
η_1^0				$\frac{15+17c_{2\theta}}{48}$	$-\sqrt{\frac{5}{3}} \frac{s_\theta^2}{4}$			
η					$-\frac{5s_\theta^2}{8}$			
η_3^+			—			$\frac{3c_\theta^2}{2}$	$-\frac{ic_\theta}{2}$	
η_5^+							$\frac{5+c_{2\theta}}{4}$	
η_5^{++}				—				c_θ^2

	$K_{AZ}^{S_i^+ S_j^-}$			$K_{AZ}^{S_i^{++} S_j^{--}}$			$K_{AW}^{S_i^0 S_j^+}$			$K_{AW}^{S_i^- S_j^{++}}$		
	η_3^-	η_5^-	η_5^{--}	η_3^+	η_5^+	η_5^{++}	η_3^+	η_5^+	η_5^{++}	η_3^+	η_5^+	η_5^{++}
η_3^+	c_{2W}	ic_θ	—				h	0	0			
η_5^+		c_{2W}					η_3^0	$-\frac{i}{2}$	$\frac{c_\theta}{2}$			
η_5^{++}		—	$4c_{2W}$				η_5^0	$-\frac{c_\theta}{2\sqrt{3}}$	$\frac{i\sqrt{3}}{2}$	—		
							η_1^0	$\sqrt{\frac{2}{3}} c_\theta$	0			
							η	0	0			
							η_3^-			$\frac{3c_\theta}{\sqrt{2}}$		
							η_5^-			$-\frac{3i}{\sqrt{2}}$		

	$K_{ZW}^{S_i^0 S_j^+}$		$K_{ZW}^{S_i^- S_j^{++}}$	$K_{W^- W^-}^{S_i^+ S_j^+}$		$K_{W^- W^-}^{S_i^0 S_j^{++}}$
	η_3^+	η_5^+	η_5^{++}	η_3^+	η_5^+	η_5^{++}
h	0	0		η_3^+	$-\frac{c_{2\theta}}{4}$	$\frac{ic_\theta}{2}$
η_3^0	$\frac{i(s_W^2 + c_{2\theta})}{2}$	$-\frac{(1+s_W^2)c_\theta}{2}$		η_5^+		$\frac{3-c_{2\theta}}{8}$
η_5^0	$-\frac{(3-s_W^2)c_\theta}{2\sqrt{3}}$	$\frac{i(3c_{2W}-c_{2\theta})}{4\sqrt{3}}$	—	h		0
η_1^0	$-\sqrt{\frac{2}{3}}s_W^2 c_\theta$	$-\frac{i(3+5c_{2\theta})}{4\sqrt{6}}$		η_3^0		$-\frac{ic_\theta}{2}$
η	0	$\sqrt{\frac{5}{2}}\frac{is_\theta^2}{2}$		η_5^0	—	$\frac{3-c_{2\theta}}{2\sqrt{6}}$
η_3^-	—		$\frac{(1-3s_W^2)c_\theta}{\sqrt{2}}$	η_1^0		$\frac{3+5c_{2\theta}}{8\sqrt{3}}$
η_5^-	—		$-\frac{i(3c_{2W}-c_{2\theta})}{2\sqrt{2}}$	η		$-\frac{\sqrt{5}s_\theta^2}{4}$

Coefficients appearing in $\mathcal{L}_{SV\tilde{V}}$

The coefficients for the anomaly terms are specified up to an overall factor coming from the dimension of the hyperfermion irrep.

	$\tilde{K}_{\gamma\gamma}^{S_i^0}$	$\tilde{K}_{\gamma Z}^{S_i^0}$	$\tilde{K}_{ZZ}^{S_i^0}$	$\tilde{K}_{W^+ W^-}^{S_i^0}$	$\tilde{K}_{\gamma W^-}^{S_i^+}$	$\tilde{K}_{ZW^-}^{S_i^+}$	$\tilde{K}_{W^- W^-}^{S_i^{++}}$
h	0	0	0	0			
η_3^0	0	0	0	0			
η_5^0	$-\frac{2s_\theta}{\sqrt{3}}$	$-\frac{c_{2W}s_\theta}{\sqrt{3}}$	$\frac{(1-3c_{4W}+2c_{2\theta})s_\theta}{12\sqrt{3}}$	$\frac{s_\theta^3}{6\sqrt{3}}$	—		
η_1^0	$\sqrt{\frac{2}{3}}s_\theta$	$\frac{c_{2W}s_\theta}{\sqrt{6}}$	$\frac{(1+6c_{4W}-7c_{2\theta})s_\theta}{24\sqrt{6}}$	$\frac{7s_\theta^3}{12\sqrt{6}}$			—
η	$\sqrt{\frac{2}{5}}s_\theta$	$\frac{c_{2W}s_\theta}{\sqrt{10}}$	$\frac{(3c_\theta^2+c_{4W})s_\theta}{4\sqrt{10}}$	$\frac{(3c_{2\theta}+5)s_\theta}{8\sqrt{10}}$			
η_3^+			—		$-\frac{s_{2\theta}}{4}$	$\frac{s_W^2 s_{2\theta}}{4}$	
η_5^+					$\frac{is_\theta}{2}$	$\frac{i(c_{2W}-c_{2\theta}-2)s_\theta}{12}$	
η_5^{++}				—			$-\frac{s_\theta^3}{3\sqrt{2}}$

References

- [1] D.B. Kaplan and H. Georgi, *SU(2) x U(1) Breaking by Vacuum Misalignment*, *Phys. Lett. B* **136** (1984) 183.
- [2] D.B. Kaplan, *Flavor at SSC energies: A New mechanism for dynamically generated fermion masses*, *Nucl. Phys. B* **365** (1991) 259.
- [3] K. Agashe, R. Contino and A. Pomarol, *The Minimal composite Higgs model*, *Nucl. Phys. B* **719** (2005) 165 [[hep-ph/0412089](#)].

- [4] R. Contino, *The Higgs as a Composite Nambu-Goldstone Boson*, in *Theoretical Advanced Study Institute in Elementary Particle Physics: Physics of the Large and the Small*, pp. 235–306, 2011, DOI [[1005.4269](#)].
- [5] B. Bellazzini, C. Csáki and J. Serra, *Composite Higgses*, *Eur. Phys. J. C* **74** (2014) 2766 [[1401.2457](#)].
- [6] G. Panico and A. Wulzer, *The Composite Nambu-Goldstone Higgs*, vol. 913, Springer (2016), [10.1007/978-3-319-22617-0](#), [[1506.01961](#)].
- [7] G. Cacciapaglia, C. Pica and F. Sannino, *Fundamental Composite Dynamics: A Review*, *Phys. Rept.* **877** (2020) 1 [[2002.04914](#)].
- [8] T. Flacke, B. Fuks, M. Kunkel and L. Panizzi, “eVLQ_S012.” <http://feynrules.irmp.ucl.ac.be/wiki/NLOModels>.
- [9] T. Flacke, B. Fuks, A. Deandrea and L. Panizzi, *FeynRules plugin for Simplified MModel Generation (FSMOG)*, **in preparation**.
- [10] R. Contino, Y. Nomura and A. Pomarol, *Higgs as a holographic pseudoGoldstone boson*, *Nucl. Phys. B* **671** (2003) 148 [[hep-ph/0306259](#)].
- [11] M. Schmaltz and D. Tucker-Smith, *Little Higgs review*, *Ann. Rev. Nucl. Part. Sci.* **55** (2005) 229 [[hep-ph/0502182](#)].
- [12] B. Holdom, *Raising the Sideways Scale*, *Phys. Rev. D* **24** (1981) 1441.
- [13] A.G. Cohen and H. Georgi, *Walking Beyond the Rainbow*, *Nucl. Phys. B* **314** (1989) 7.
- [14] J. Barnard, T. Gherghetta and T.S. Ray, *UV descriptions of composite Higgs models without elementary scalars*, *JHEP* **02** (2014) 002 [[1311.6562](#)].
- [15] G. Ferretti and D. Karateev, *Fermionic UV completions of Composite Higgs models*, *JHEP* **03** (2014) 077 [[1312.5330](#)].
- [16] M.J. Dugan, H. Georgi and D.B. Kaplan, *Anatomy of a Composite Higgs Model*, *Nucl. Phys. B* **254** (1985) 299.
- [17] G. Ferretti, *UV Completions of Partial Compositeness: The Case for a $SU(4)$ Gauge Group*, *JHEP* **06** (2014) 142 [[1404.7137](#)].
- [18] J. Galloway, J.A. Evans, M.A. Luty and R.A. Tacchi, *Minimal Conformal Technicolor and Precision Electroweak Tests*, *JHEP* **10** (2010) 086 [[1001.1361](#)].
- [19] G. Cacciapaglia and F. Sannino, *Fundamental Composite (Goldstone) Higgs Dynamics*, *JHEP* **04** (2014) 111 [[1402.0233](#)].
- [20] T. Ma and G. Cacciapaglia, *Fundamental Composite 2HDM: $SU(N)$ with 4 flavours*, *JHEP* **03** (2016) 211 [[1508.07014](#)].

- [21] Y. Wu, T. Ma, B. Zhang and G. Cacciapaglia, *Composite Dark Matter and Higgs*, *JHEP* **11** (2017) 058 [[1703.06903](#)].
- [22] J. Mrazek, A. Pomarol, R. Rattazzi, M. Redi, J. Serra and A. Wulzer, *The Other Natural Two Higgs Doublet Model*, *Nucl. Phys. B* **853** (2011) 1 [[1105.5403](#)].
- [23] G. Ferretti, *Gauge theories of Partial Compositeness: Scenarios for Run-II of the LHC*, *JHEP* **06** (2016) 107 [[1604.06467](#)].
- [24] L. Vecchi, *A dangerous irrelevant UV-completion of the composite Higgs*, *JHEP* **02** (2017) 094 [[1506.00623](#)].
- [25] D. Elander, M. Frigerio, M. Knecht and J.-L. Kneur, *Holographic models of composite Higgs in the Veneziano limit. Part I. Bosonic sector*, *JHEP* **03** (2021) 182 [[2011.03003](#)].
- [26] J. Erdmenger, N. Evans, W. Porod and K.S. Rigatos, *Gauge/gravity dynamics for composite Higgs models and the top mass*, *Phys. Rev. Lett.* **126** (2021) 071602 [[2009.10737](#)].
- [27] J. Erdmenger, N. Evans, W. Porod and K.S. Rigatos, *Gauge/gravity dual dynamics for the strongly coupled sector of composite Higgs models*, *JHEP* **02** (2021) 058 [[2010.10279](#)].
- [28] D. Elander, M. Frigerio, M. Knecht and J.-L. Kneur, *Holographic models of composite Higgs in the Veneziano limit: 2. Fermionic sector*, [2112.14740](#).
- [29] T. Gherghetta and M.D. Nguyen, *A Composite Higgs with a Heavy Composite Axion*, *JHEP* **12** (2020) 094 [[2007.10875](#)].
- [30] T. Appelquist, J. Ingoldby and M. Piai, *Nearly Conformal Composite Higgs Model*, *Phys. Rev. Lett.* **126** (2021) 191804 [[2012.09698](#)].
- [31] G. Cacciapaglia, S. Vatani and C. Zhang, *Composite Higgs Meets Planck Scale: Partial Compositeness from Partial Unification*, *Phys. Lett. B* **815** (2021) 136177 [[1911.05454](#)].
- [32] N. Bizot, M. Frigerio, M. Knecht and J.-L. Kneur, *Nonperturbative analysis of the spectrum of meson resonances in an ultraviolet-complete composite-Higgs model*, *Phys. Rev. D* **95** (2017) 075006 [[1610.09293](#)].
- [33] M. Montull, F. Riva, E. Salvioni and R. Torre, *Higgs Couplings in Composite Models*, *Phys. Rev. D* **88** (2013) 095006 [[1308.0559](#)].
- [34] V. Sanz and J. Setford, *Composite Higgs Models after Run 2*, *Adv. High Energy Phys.* **2018** (2018) 7168480 [[1703.10190](#)].
- [35] D. Liu, I. Low and C.E.M. Wagner, *Modification of Higgs Couplings in Minimal Composite Models*, *Phys. Rev. D* **96** (2017) 035013 [[1703.07791](#)].

- [36] A. Banerjee, G. Bhattacharyya, N. Kumar and T.S. Ray, *Constraining Composite Higgs Models using LHC data*, *JHEP* **03** (2018) 062 [[1712.07494](#)].
- [37] D. Liu, I. Low and Z. Yin, *Universal Relations in Composite Higgs Models*, *JHEP* **05** (2019) 170 [[1809.09126](#)].
- [38] A. Arbey, G. Cacciapaglia, H. Cai, A. Deandrea, S. Le Corre and F. Sannino, *Fundamental Composite Electroweak Dynamics: Status at the LHC*, *Phys. Rev. D* **95** (2017) 015028 [[1502.04718](#)].
- [39] A. Belyaev, G. Cacciapaglia, H. Cai, G. Ferretti, T. Flacke, A. Parolini et al., *Di-boson signatures as Standard Candles for Partial Compositeness*, *JHEP* **01** (2017) 094 [[1610.06591](#)].
- [40] A. Agugliaro, G. Cacciapaglia, A. Deandrea and S. De Curtis, *Vacuum misalignment and pattern of scalar masses in the $SU(5)/SO(5)$ composite Higgs model*, *JHEP* **02** (2019) 089 [[1808.10175](#)].
- [41] G. Cacciapaglia, H. Cai, A. Deandrea, T. Flacke, S.J. Lee and A. Parolini, *Composite scalars at the LHC: the Higgs, the Sextet and the Octet*, *JHEP* **11** (2015) 201 [[1507.02283](#)].
- [42] N. Bizot, G. Cacciapaglia and T. Flacke, *Common exotic decays of top partners*, *JHEP* **06** (2018) 065 [[1803.00021](#)].
- [43] G. Cacciapaglia, T. Flacke, M. Park and M. Zhang, *Exotic decays of top partners: mind the search gap*, *Phys. Lett. B* **798** (2019) 135015 [[1908.07524](#)].
- [44] K.-P. Xie, G. Cacciapaglia and T. Flacke, *Exotic decays of top partners with charge 5/3: bounds and opportunities*, *JHEP* **10** (2019) 134 [[1907.05894](#)].
- [45] O. Matsedonskyi, F. Riva and T. Vantalón, *Composite Charge 8/3 Resonances at the LHC*, *JHEP* **04** (2014) 059 [[1401.3740](#)].
- [46] G. Corcella, A. Costantini, M. Ghezzi, L. Panizzi, G.M. Pruna and J. Šalko, *Vector-like quarks decaying into singly and doubly charged bosons at LHC*, *JHEP* **10** (2021) 108 [[2107.07426](#)].
- [47] S. Dasgupta, R. Pramanick and T.S. Ray, *Broad top-like vector quarks at LHC and HL-LHC*, [2112.03742](#).
- [48] M. Chala, *Direct bounds on heavy toplike quarks with standard and exotic decays*, *Phys. Rev. D* **96** (2017) 015028 [[1705.03013](#)].
- [49] G. Cacciapaglia, T. Flacke, M. Kunkel and W. Porod, *Phenomenology of unusual top partners in composite Higgs models*, *JHEP* **02** (2022) 208 [[2112.00019](#)].
- [50] A. Azatov, D. Chowdhury, D. Ghosh and T.S. Ray, *Same sign di-lepton candles of the composite gluons*, *JHEP* **08** (2015) 140 [[1505.01506](#)].

- [51] D. Buarque Franzosi, G. Cacciapaglia, H. Cai, A. Deandrea and M. Frandsen, *Vector and Axial-vector resonances in composite models of the Higgs boson*, *JHEP* **11** (2016) 076 [[1605.01363](#)].
- [52] J. Yepes and A. Zerwekh, *Modelling top partner-vector resonance phenomenology*, *Nucl. Phys. B* **941** (2019) 560 [[1806.06694](#)].
- [53] S. Dasgupta, S.K. Rai and T.S. Ray, *Impact of a colored vector resonance on the collider constraints for top-like top partner*, *Phys. Rev. D* **102** (2020) 115014 [[1912.13022](#)].
- [54] A. Banerjee, S. Dasgupta and T.S. Ray, *Probing composite Higgs boson substructure at the HL-LHC*, *Phys. Rev. D* **104** (2021) 095021 [[2105.01093](#)].
- [55] G. Cacciapaglia, G. Ferretti, T. Flacke and H. Serôdio, *Light scalars in composite Higgs models*, *Front. in Phys.* **7** (2019) 22 [[1902.06890](#)].
- [56] D. Buarque Franzosi, G. Cacciapaglia, X. Cid Vidal, G. Ferretti, T. Flacke and C. Vázquez Sierra, *Exploring new possibilities to discover a light pseudo-scalar at LHCb*, *Eur. Phys. J. C* **82** (2022) 3 [[2106.12615](#)].
- [57] S.R. Coleman, J. Wess and B. Zumino, *Structure of phenomenological Lagrangians. 1.*, *Phys. Rev.* **177** (1969) 2239.
- [58] C.G. Callan, Jr., S.R. Coleman, J. Wess and B. Zumino, *Structure of phenomenological Lagrangians. 2.*, *Phys. Rev.* **177** (1969) 2247.
- [59] A. De Simone, O. Matsedonskyi, R. Rattazzi and A. Wulzer, *A First Top Partner Hunter's Guide*, *JHEP* **04** (2013) 004 [[1211.5663](#)].
- [60] D. Marzocca, M. Serone and J. Shu, *General Composite Higgs Models*, *JHEP* **08** (2012) 013 [[1205.0770](#)].
- [61] A. Banerjee, D. Buarque Franzosi and G. Ferretti, *Modelling vector-like quarks in partial compositeness framework*, [2202.00037](#).
- [62] C. Degrande, C. Duhr, B. Fuks, D. Grellscheid, O. Mattelaer and T. Reiter, *UFO - The Universal FeynRules Output*, *Comput. Phys. Commun.* **183** (2012) 1201 [[1108.2040](#)].
- [63] ATLAS collaboration, *Search for doubly and singly charged Higgs bosons decaying into vector bosons in multi-lepton final states with the ATLAS detector using proton-proton collisions at $\sqrt{s} = 13$ TeV*, *JHEP* **06** (2021) 146 [[2101.11961](#)].
- [64] ATLAS collaboration, *Measurement of the $Z(\rightarrow \ell^+\ell^-)\gamma$ production cross-section in pp collisions at $\sqrt{s} = 13$ TeV with the ATLAS detector*, *JHEP* **03** (2020) 054 [[1911.04813](#)].
- [65] ATLAS collaboration, *Measurement of the production cross section of pairs of isolated photons in pp collisions at 13 TeV with the ATLAS detector*, *JHEP* **11** (2021) 169 [[2107.09330](#)].

- [66] ATLAS collaboration, *Measurement of the $Z\gamma \rightarrow \nu\bar{\nu}\gamma$ production cross section in pp collisions at $\sqrt{s} = 13$ TeV with the ATLAS detector and limits on anomalous triple gauge-boson couplings*, *JHEP* **12** (2018) 010 [[1810.04995](#)].
- [67] ATLAS collaboration, *Measurements of differential cross-sections in four-lepton events in 13 TeV proton-proton collisions with the ATLAS detector*, *JHEP* **07** (2021) 005 [[2103.01918](#)].
- [68] ATLAS collaboration, *Measurements of $W^+W^- + \geq 1$ jet production cross-sections in pp collisions at $\sqrt{s} = 13$ TeV with the ATLAS detector*, *JHEP* **06** (2021) 003 [[2103.10319](#)].
- [69] ATLAS collaboration, *Searches for scalar leptoquarks and differential cross-section measurements in dilepton-dijet events in proton-proton collisions at a centre-of-mass energy of $\sqrt{s} = 13$ TeV with the ATLAS experiment*, *Eur. Phys. J. C* **79** (2019) 733 [[1902.00377](#)].
- [70] CMS collaboration, *Measurements of differential Z boson production cross sections in proton-proton collisions at $\sqrt{s} = 13$ TeV*, *JHEP* **12** (2019) 061 [[1909.04133](#)].
- [71] A. Alloul, N.D. Christensen, C. Degrande, C. Duhr and B. Fuks, *FeynRules 2.0 - A complete toolbox for tree-level phenomenology*, *Comput. Phys. Commun.* **185** (2014) 2250 [[1310.1921](#)].
- [72] J. Alwall, R. Frederix, S. Frixione, V. Hirschi, F. Maltoni, O. Mattelaer et al., *The automated computation of tree-level and next-to-leading order differential cross sections, and their matching to parton shower simulations*, *JHEP* **07** (2014) 079 [[1405.0301](#)].
- [73] R.D. Ball et al., *Parton distributions with LHC data*, *Nucl. Phys. B* **867** (2013) 244 [[1207.1303](#)].
- [74] A. Buckley, J. Ferrando, S. Lloyd, K. Nordström, B. Page, M. Rüfenacht et al., *LHAPDF6: parton density access in the LHC precision era*, *Eur. Phys. J. C* **75** (2015) 132 [[1412.7420](#)].
- [75] T. Sjöstrand, S. Ask, J.R. Christiansen, R. Corke, N. Desai, P. Ilten et al., *An introduction to PYTHIA 8.2*, *Comput. Phys. Commun.* **191** (2015) 159 [[1410.3012](#)].
- [76] E. Conte, B. Fuks and G. Serret, *MadAnalysis 5, A User-Friendly Framework for Collider Phenomenology*, *Comput.Phys.Commun.* **184** (2013) 222 [[1206.1599](#)].
- [77] E. Conte, B. Dumont, B. Fuks and C. Wymant, *Designing and recasting LHC analyses with MadAnalysis 5*, *Eur. Phys. J. C* **74** (2014) 3103 [[1405.3982](#)].
- [78] B. Dumont, B. Fuks, S. Kraml, S. Bein, G. Chalons et al., *Toward a public analysis database for LHC new physics searches using MADANALYSIS 5*, *Eur.Phys.J. C* **75** (2015) 56 [[1407.3278](#)].

- [79] E. Conte and B. Fuks, *Confronting new physics theories to LHC data with MADANALYSIS 5*, *Int. J. Mod. Phys. A* **33** (2018) 1830027 [[1808.00480](#)].
- [80] DELPHES 3 collaboration, *DELPHES 3, A modular framework for fast simulation of a generic collider experiment*, *JHEP* **02** (2014) 057 [[1307.6346](#)].
- [81] M. Cacciari, G.P. Salam and G. Soyez, *The anti- k_t jet clustering algorithm*, *JHEP* **04** (2008) 063 [[0802.1189](#)].
- [82] M. Cacciari, G.P. Salam and G. Soyez, *FastJet User Manual*, *Eur. Phys. J. C* **72** (2012) 1896 [[1111.6097](#)].
- [83] A.L. Read, *Presentation of search results: The $CL(s)$ technique*, *J. Phys. G* **28** (2002) 2693.
- [84] C. Bierlich et al., *Robust Independent Validation of Experiment and Theory: Rivet version 3*, *SciPost Phys.* **8** (2020) 026 [[1912.05451](#)].
- [85] J. Butterworth, *BSM constraints from model-independent measurements: A Contur Update*, *J. Phys. Conf. Ser.* **1271** (2019) 012013 [[1902.03067](#)].
- [86] A. Buckley et al., *Testing new physics models with global comparisons to collider measurements: the Contur toolkit*, *SciPost Phys. Core* **4** (2021) 013 [[2102.04377](#)].
- [87] ATLAS collaboration, *Observation of electroweak production of a same-sign W boson pair in association with two jets in pp collisions at $\sqrt{s} = 13$ TeV with the ATLAS detector*, *Phys. Rev. Lett.* **123** (2019) 161801 [[1906.03203](#)].
- [88] M. Drees, H. Dreiner, D. Schmeier, J. Tattersall and J.S. Kim, *CheckMATE: Confronting your Favourite New Physics Model with LHC Data*, *Comput. Phys. Commun.* **187** (2015) 227 [[1312.2591](#)].
- [89] D. Dercks, N. Desai, J.S. Kim, K. Rolbiecki, J. Tattersall and T. Weber, *CheckMATE 2: From the model to the limit*, *Comput. Phys. Commun.* **221** (2017) 383 [[1611.09856](#)].
- [90] CMS collaboration, *Search for production of four top quarks in final states with same-sign or multiple leptons in proton-proton collisions at $\sqrt{s} = 13$ TeV*, *Eur. Phys. J. C* **80** (2020) 75 [[1908.06463](#)].
- [91] L. Darmé and B. Fuks, *Implementation of the CMS-TOP-18-003 analysis in the MadAnalysis 5 framework (four top quarks with at least two leptons; $137/\text{fb}$)*, *Mod. Phys. Lett. A* **36** (2021) 2141008.
- [92] CMS collaboration, *Search for pair production of vector-like quarks in the $bW\bar{b}W$ channel from proton-proton collisions at $\sqrt{s} = 13$ TeV*, *Phys. Lett. B* **779** (2018) 82 [[1710.01539](#)].
- [93] ATLAS collaboration, *Search for new phenomena in events with same-charge leptons and b -jets in pp collisions at $\sqrt{s} = 13$ TeV with the ATLAS detector*, *JHEP* **12** (2018) 039 [[1807.11883](#)].

- [94] ATLAS collaboration, *Search for pair production of up-type vector-like quarks and for four-top-quark events in final states with multiple b-jets with the ATLAS detector*, *JHEP* **07** (2018) 089 [[1803.09678](#)].
- [95] ATLAS collaboration, *Search for pair production of heavy vector-like quarks decaying into high- p_T W bosons and top quarks in the lepton-plus-jets final state in pp collisions at $\sqrt{s} = 13$ TeV with the ATLAS detector*, *JHEP* **08** (2018) 048 [[1806.01762](#)].
- [96] ATLAS collaboration, *Search for pair production of heavy vector-like quarks decaying to high- p_T W bosons and b quarks in the lepton-plus-jets final state in pp collisions at $\sqrt{s} = 13$ TeV with the ATLAS detector*, *JHEP* **10** (2017) 141 [[1707.03347](#)].
- [97] ATLAS collaboration, *Search for pair- and single-production of vector-like quarks in final states with at least one Z boson decaying into a pair of electrons or muons in pp collision data collected with the ATLAS detector at $\sqrt{s} = 13$ TeV*, *Phys. Rev. D* **98** (2018) 112010 [[1806.10555](#)].
- [98] ATLAS collaboration, *Search for pair production of heavy vector-like quarks decaying into hadronic final states in pp collisions at $\sqrt{s} = 13$ TeV with the ATLAS detector*, *Phys. Rev. D* **98** (2018) 092005 [[1808.01771](#)].
- [99] ATLAS collaboration, *Search for pair production of vector-like top quarks in events with one lepton, jets, and missing transverse momentum in $\sqrt{s} = 13$ TeV pp collisions with the ATLAS detector*, *JHEP* **08** (2017) 052 [[1705.10751](#)].
- [100] ATLAS collaboration, *Combination of the searches for pair-produced vector-like partners of the third-generation quarks at $\sqrt{s} = 13$ TeV with the ATLAS detector*, *Phys. Rev. Lett.* **121** (2018) 211801 [[1808.02343](#)].
- [101] CMS collaboration, *Search for vector-like T and B quark pairs in final states with leptons at $\sqrt{s} = 13$ TeV*, *JHEP* **08** (2018) 177 [[1805.04758](#)].
- [102] CMS collaboration, *Combination of CMS searches for heavy resonances decaying to pairs of bosons or leptons*, *Phys. Lett. B* **798** (2019) 134952 [[1906.00057](#)].
- [103] CMS collaboration, *A search for bottom-type, vector-like quark pair production in a fully hadronic final state in proton-proton collisions at $\sqrt{s} = 13$ TeV*, *Phys. Rev. D* **102** (2020) 112004 [[2008.09835](#)].
- [104] S. Banerjee, D. Barducci, G. Bélanger and C. Delaunay, *Implications of a High-Mass Diphoton Resonance for Heavy Quark Searches*, *JHEP* **11** (2016) 154 [[1606.09013](#)].
- [105] M. Chala, R. Gröber and M. Spannowsky, *Searches for vector-like quarks at future colliders and implications for composite Higgs models with dark matter*, *JHEP* **03** (2018) 040 [[1801.06537](#)].
- [106] R. Benbrik et al., *Signatures of vector-like top partners decaying into new neutral scalar or pseudoscalar bosons*, *JHEP* **05** (2020) 028 [[1907.05929](#)].

- [107] M. Ramos, *Composite dark matter phenomenology in the presence of lighter degrees of freedom*, *JHEP* **07** (2020) 128 [[1912.11061](#)].
- [108] J.A. Aguilar-Saavedra, J. Alonso-González, L. Merlo and J.M. No, *Exotic vectorlike quark phenomenology in the minimal linear σ model*, *Phys. Rev. D* **101** (2020) 035015 [[1911.10202](#)].
- [109] G. Brooijmans et al., *Les Houches 2019 Physics at TeV Colliders: New Physics Working Group Report*, in *11th Les Houches Workshop on Physics at TeV Colliders: PhysTeV Les Houches*, 2, 2020 [[2002.12220](#)].
- [110] D. Wang, L. Wu and M. Zhang, *Hunting for top partner with a new signature at the LHC*, *Phys. Rev. D* **103** (2021) 115017 [[2007.09722](#)].
- [111] R. Dermisek, E. Lunghi, N. McGinnis and S. Shin, *Signals with six bottom quarks for charged and neutral Higgs bosons*, *JHEP* **07** (2020) 241 [[2005.07222](#)].
- [112] R. Dermisek, E. Lunghi, N. McGinnis and S. Shin, *Tau-jet signatures of vectorlike quark decays to heavy charged and neutral Higgs bosons*, *JHEP* **08** (2021) 159 [[2105.10790](#)].
- [113] A. Roy, N. Nikiforou, N. Castro and T. Andeen, *Novel interpretation strategy for searches of singly produced vectorlike quarks at the LHC*, *Phys. Rev. D* **101** (2020) 115027 [[2003.00640](#)].
- [114] CMS collaboration, *Search for top quark partners with charge 5/3 in the same-sign dilepton and single-lepton final states in proton-proton collisions at $\sqrt{s} = 13$ TeV*, *JHEP* **03** (2019) 082 [[1810.03188](#)].
- [115] D. Barducci and L. Panizzi, *Vector-like quarks coupling discrimination at the LHC and future hadron colliders*, *JHEP* **12** (2017) 057 [[1710.02325](#)].
- [116] L. Li, Y.-Y. Li and T. Liu, *Anatomy of $t\bar{t}hh$ physics at the HL-LHC*, *Phys. Rev. D* **101** (2020) 055043 [[1905.03772](#)].
- [117] ALEPH, DELPHI, L3, OPAL, LEP collaboration, *Search for Charged Higgs bosons: Combined Results Using LEP Data*, *Eur. Phys. J. C* **73** (2013) 2463 [[1301.6065](#)].
- [118] ATLAS collaboration, *Search for doubly charged Higgs boson production in multi-lepton final states with the ATLAS detector using proton-proton collisions at $\sqrt{s} = 13$ TeV*, *Eur. Phys. J. C* **78** (2018) 199 [[1710.09748](#)].
- [119] V. Ayyar, T. Degrand, D.C. Hackett, W.I. Jay, E.T. Neil, Y. Shamir et al., *Baryon spectrum of $SU(4)$ composite Higgs theory with two distinct fermion representations*, *Phys. Rev. D* **97** (2018) 114505 [[1801.05809](#)].
- [120] V. Ayyar, T. DeGrand, D.C. Hackett, W.I. Jay, E.T. Neil, Y. Shamir et al., *Partial compositeness and baryon matrix elements on the lattice*, *Phys. Rev. D* **99** (2019) 094502 [[1812.02727](#)].